Sains Malaysiana 39(6)(2010): 1007–1013

Dependence of Pyroelectric Properties of $La_{0.03}Sr_{0.255}Ba_{0.7}Nb_{2-y}Ti_yO_{(6-y/2)}$ Ceramic on Electric Field, Grain Refinement and Ti/Nb Crystallite Sizes

(Kebergantungan Sifat Piroelektrik Seramik $La_{0.03}Sr_{0.255}Ba_{0.7}Nb_{2-y}Ti_yO_{(6-y/2)}$ Terhadap Medan Elektrik dan Saiz Hablur Ti/Nb)

WEE CHEN GAN* & WAN HALIZA ABD. MAJID

ABSTRACT

The pyroelectric properties of $La_{0.03}Sr_{0.255}Ba_{0.7}Nb_{2-y}Ti_yO_{(6-y/2)}$ (LSBNT) ceramic pellets using several Ti/Nb ratios sintered at 1250°C for 5 h were investigated. The samples were subjected to several values of electric fields in order to obtain the optimum electric field strength. The pyroelectric coefficients, (p) were measured using the quasi-static method by applying several heating rates. The results show that the Ti/Nb ratios and the dc poling field, (E_{dc}) influenced the measured pyroelectric coefficient of the LSBNT ceramic pellets. The mean grain size of the particles as obtained from scanning electron microscope (SEM) does not seem to give significant impact on the pyroelectric coefficient of the ceramic pellets. However, the X-Ray diffraction (XRD) results indicate that the crystallite sizes of Ti and Nb of these ceramic pellets after being treated with sintering process also influence the measured pyroelectric coefficients of the ceramic pellets.

Keywords: Ferroelectric ceramic; pyroelectric; spontaneous polarization

ABSTRAK

Sifat piroelektrik $La_{0.03}Sr_{0.255}Ba_{0.7}Nb_{2-y}Ti_yO_{(6-y/2)}$ (LSBNT) pelet seramik dengan nisbah Ti/Nb yang berlainan selepas dipanaskan pada suhu 1250°C selama 5 jam telah dikaji. Sampel dikenakan medan elektrik yang berlainan supaya ia mencapai keadaan medan elektrik yang optimum. Pekali piroelektrik, (p) ditentukan dengan menggunakan kaedah kuasi-statik. Keputusan yang didapati menunjukkan nisbah Ti/Nb dan medan kutub arus terus, (E_{dc}) mempengaruhi pekali piroelektrik seramik LSBNT yang dikaji. Saiz butiran seperti yang didapati daripada mikroskop imbiasan elektron (SEM) tidak menunjukkan sebarang pengaruh yang ketara terhadap pekalian piroelektrik seramik. Bagaimanapun, keputusan pembiasan sinar-X (XRD) yang diperolehi menunjukkan saiz hablur Ti dan Nb seramik yang telah dirawat dengan proses pemanasan menpengaruhi pekali piroelektrik seramik.

Kata kunci: Pengutuban spontan; piroelektrik; seramik feroelektrik

INTRODUCTION

Pyroelectricity is one of the occasional properties of some ferroelectric solid materials. Pyroelectricity is the effect of the generation of spontaneous polarization in certain anisotropic solids with the change of temperature. Spontaneous polarization in the dielectric crystal in the absence of an electric field is the dipole moment per unit volume of the pyroelectric materials. The dipole moment per unit volume has to be non-zero and it must be equal to the layer of bound charge on each flat surface of the sample in order to observe pyroelectric activity. As the temperature changes, a variation of the charge density can be observed on those surfaces of the sample which are perpendicular to the unique polar axis in the crystal. The change in temperature alters the spontaneous polarization in such a way as to increase or decrease, and lead to the so called pyroelectricity flow (Lang 2005; Xu 1991).

Pyroelectric materials have been widely used as temperature sensors and IR-light detectors due to their wide bandwidth, fast electromechanical response, relatively low power requirements and high generative forces (Harrison & Ounaies 2001). The niobate crystals with tungsten-bronze structure such as $Sr_xBa_{1-x}Nb_2O_6$ (SBN) system are one of the outstanding ferroelectric materials which exhibit high pyroelectric and electro-optic coefficients and low dielectric permittivity (Amorin et al. 2000b). $Sr_{0.5}Ba_{0.5}Nb_2O_6$ (SBN 50/50) system is the most investigated composition due to its excellent dielectric properties at room temperature (Amorin et al. 2000a; Perez et al. 2001).

Recently, there are few reports which indicate that doping of certain rare earth elements in the SBN system will lead to lower Curie temperature (T_c) and improves the dielectric and pyroelectric of the system properties at room temperature. The physical properties are modified according to the cationic substitution (Maciolek & Liu 1975; Nagata et al. 1981). A modified SBN ceramic doped with lanthanum and titanium, as $La_{0.03}Sr_{0.255}Ba_{0.7}Nb_{2-y}Ti_yO_{(6-y/2)}$ (LSBNT) ceramic has been investigated by Amorin et al. (1999). The doping of lanthanum in this ceramic produces a very stable polarized material at room temperature (Liu

& Bhalla 1983). However, the presence of a small amount of titanium enhances the dipolar mechanisms activation (Amorin et al. 1999). A significant dielectric, ferroelectric and pyroelctric effects are to be expected when niobium is substituted by titanium. The ferroactive ion is being partially substituted and a 5+ valence ion (Nb) is replaced by a 4+ valence ion (Ti). Vacancies in the oxygen sites appear to maintain charge neutrality and thus increasing the number of defects in the structure, leading to a decrease in the transition temperature of the sample (Amorin et al. 1999).

Amorin et al. (2000b) reported the pyroelectric activity of some LSBNT systems. The pyroelectric activity of LSBNT system depends on the Ti concentration. The Ti concentration is also reported to influence the mean grain size of the LSBNT ceramic. This study, however, is mainly focused on the influence of the grain size on the pyroelectric properties of LSBNT samples as heated at intermediate sintering phase. Sintering itself has three predominant stages, called initial, intermediate and final stages. Amorin et al. (2000b) mainly focus on final stage of sintering process where the densification and crystal grain size reach its maximum value. These works at the final sintering stage have been well explored. The electrical properties of LSBNT ceramic under sintered at the intermediate temperature phase (1250°C), however, have not been thoroughly reviewed. Ares et al. (2005) pointed out that the crystallite size is usually measured from X-ray diffraction patterns and grain size by other experimental techniques like scanning electron microscope (Okada et al. 2003; Xu et al. 2004), scanning tunneling microscopy (Leite et al. 2004) or atomic force microscopy (Calzada et al. 2004) depending on the type and characteristic of the material. Thus, in this article, the influence of grain size on the pyroelectric properties of LSBNT samples heated at the intermediate sintering phase is reported. The pyroelectric activities of $La_{0.03}Sr_{0.255}Ba_{0.7}Nb_{2-y}Ti_yO_{(6-y/2)}$ (LSBNT) ceramic pellets with several Ti/Nb concentrations were investigated. The samples were subjected to different values of electric field, (E_{dc}) by quasi-static method. The effects of grain size on the pyroelectric coefficient of the ceramic were studied from the scanning electron micrographs while that of Ti and Nb crystallite sizes were investigated by the X-Ray diffraction method.

Experimental Details

$BaCO_3$, $SrCO_3$, La_2O_3, Nb_2O_5 and TiO_2 with high purity grade (>99.9%) were purchased from Sigma-Aldrich to prepare $La_{0.03}Sr_{0.255}Ba_{0.7}Nb_{2-y}TiyO_{(6-y/2)}$ (LSBNT) ceramic pellets. The samples with different Ti and Nb ratios were prepared to examine the pyroelectric activity. The five different concentrations used were $y = 0.01$ (LSBNT 1), $y = 0.03$ (LSBNT 3), $y = 0.05$ (LSBNT 5), $y = 0.07$ (LSBNT 7) and $y = 0.10$ (LSBNT 10). Initially, the powders were mixed together and heated at 1100°C for 2 h. After the heating process, the powders were die-pressed at 8 tonnes, into 13 mm diameter discs. Subsequently, the samples were sintered at 1250°C for 5 h. Aluminium were then thermally evaporated on both sides of the ceramic samples as the conducting electrodes. The LSBNT samples were poled for 1 hour at room temperature by applying a range of constant high electric field in order to attain the pyroelectric activity. The poling electric field used was in the range of 10 to 30 kV cm^{-1}. The samples were broken down when the poling field was above 30 kV cm^{-1} as shown in Figure 1, where no pyroelectric current was detected.

In the quasi-static method, the generated short-circuited pyroelectricity was measured as a triangular waveform temperature with different heating rates applied to the sample. The temperature of the sample was set to increase at a constant rate in order to generate a triangle temperature waveform while recording the pyroelectricity. The principal formula which has been used to determine the pyroelectric coefficient is,

$$I_p = pA\frac{dT}{dt} \tag{1}$$

where p is the pyroelectric coefficient, I_p is the pyroelectric current, A is the effective area of the sample and dT/dt is the rate of temperature change. The samples were examined by X-ray diffractometer (Siemens D5000) to identify the crystallite phases. The means crystallite size, D was obtained from the Scherrer's equation (Rittidech & Khotsongkram 2006):

$$D = \frac{k\lambda}{\beta\cos\theta} \tag{2}$$

where $k = 0.9$, $\lambda = 1.541$, θ is the diffraction peak angle and β denotes the full width at half maximum of the corresponding diffraction peak. The grain sizes and morphologies of the ceramics were obtained by scanning electron microscope (SEM).

Results and Discussions

An ideal square pyroelectric waveform was observed for sample LSBNT 7 at the heating rate of 0.15°C s^{-1} as shown in Figure 2. The sample was previously poled at 20 kV cm^{-1}. These results coincide with the pyroelectric definition which states that when certain materials experience a temperature gradient, a short circuit pyroelectric current due to the change of electric dipole moment is generated. When the heat is absorbed or vibrated, the dipoles fixed about their mean positions which are perpendicular to the unique polar axis in the crystal vibrate and alter to the opposite direction as shown in Figure 3. Therefore, as a triangular temperature waveform is applied to the sample, the square pyroelectric waveform is expected to form (Abd. Majid 1994). Figure 4 shows the peak-to-peak current, (I_{p-p}) plotted as a function of total rate of temperature change, dT/dt (°C/s) for LSBNT 7 which has been previously poled at 20 kV cm^{-1}. The figure indicates that higher rate of temperature change or heat transfers on the samples are important to

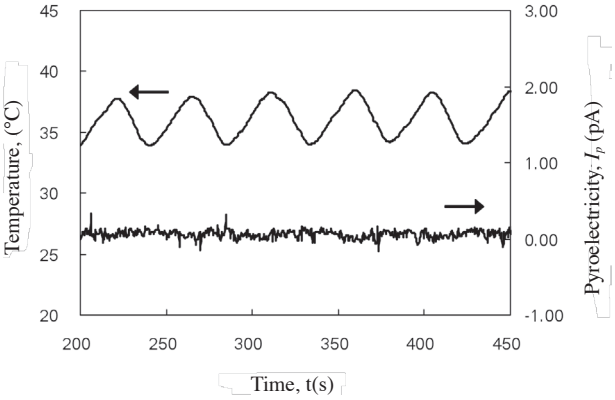

FIGURE 1. No pyroelectricity is observed as the sample being poled at 30 kV cm^{-1}

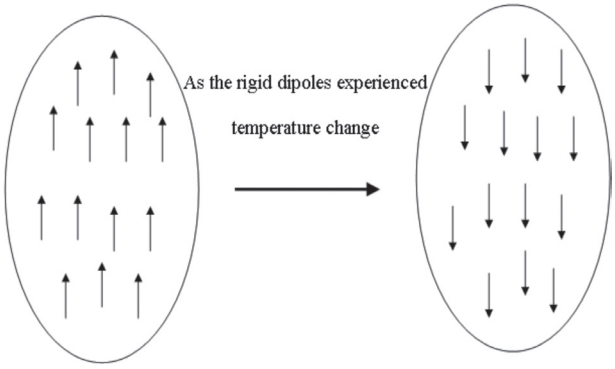

FIGURE 3. Illustration of rigid dipoles motion as it experienced temperature change

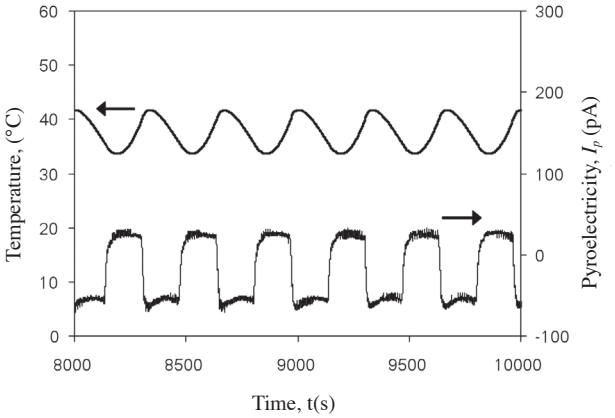

FIGURE 2. Measurement of the pyroelectric current for LSBNT 7 at the heating rate of 0.15°C/s which was previously poled at 20 kV cm^{-1}

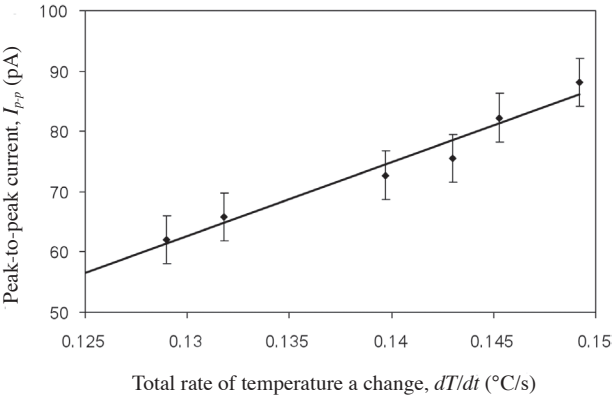

FIGURE 4. The peak-to-peak current, Ip-p is plotted as a function of total rate of temperature change, dT/dt for LSBNT 7 which was previously poled at 20 kV cm^{-1}

obtain higher peak-to-peak current. Higher temperature change also allows a quick response of the samples to reach the greatest discharge state (Kouchachvili & Ikura 2007). As a result, the pyroelectric activity observed tends to form a linear relationship between I_{p-p} and dT/dt.

A dc poling field has been applied to the LSBNT samples in order to attain the pyroelectric activity. Different values of dc poling field, (E_{dc}), have been used and as a result the samples exhibit several pyroelectric coefficients, (p) corresponding to the electric fields (10 to 30 kV cm^{-1}) as shown in Figure 5. The poling process realigns the polar axes of the crystallites and as a result, a polarization field exists inside the samples.

From Figure 5, it can also be seen that sample LSBNT 5 (with Ti concentration y = 0.05) exhibits the highest pyroelectric coefficient, $p \approx 32$ μcm^{-2}K^{-1} when the E_{dc} applied is 20 kV cm^{-1}. However, as the E_{dc} on the sample (LSBNT 5) is increased above 20 kV cm^{-1}, the pyroelectric coefficient does not seem to improve. The samples with Ti concentration, $y < 0.05$ (LSBNT 1, 3) exhibited very low pyroelectric coefficient, $p < 8$ μcm^{-2}K^{-1} for the entire range of electric field applied from 10-30 kV cm^{-1}. However, for the samples with Ti concentration, $y > 0.05$ (LSBNT 7, 10) a higher range of pyroelectric coefficient was obtained (20-27 μcm^{-2}K^{-1}). It is important to note that the poling process for sample LSBNT 7 and LSBNT 10 was performed up to 25 kV cm^{-1}. Higher electric field damages the samples due to high dipole moment or high conductivity characteristic of Ti inside the samples. The results indicate that the saturation of pyroelectric coefficient could not be reached probably due to the dielectric breakdown potential was lower than the saturation field (Amorin et al. 2000b).

The substitution of Nb by Ti also enhances the polarization of the samples with ($y \leq 0.07$) below the maximum applied electric field $E_{dc} \leq 25$ kV cm^{-1}. The high doping of Ti concentration in LSBNT 10 decreased the polarization inside the sample due to the presence of a new segregated phase that deteriorates the dielectric properties of the material, as reported by Amorin et al. (1999). In fact, the increase in Ti concentration not only lowered the polarization, but also lowered the total dipole moment per unit volume of the material and the ferroelectric-paraelectric transition temperature, T_c. Even though T_c decreases may enhance the ferroelectric and pyroelectric activities of the samples at room temperature, the dipole moment per unit volume also decreases and reduces the

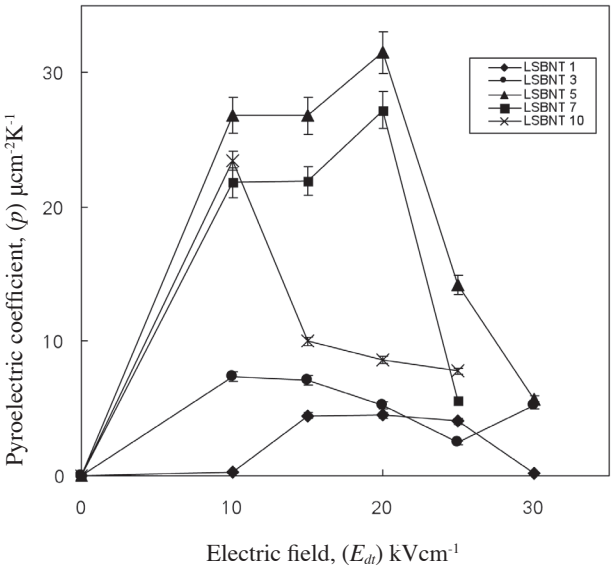

FIGURE 5. The dependence of pyroelectric coefficient, p of LSBNT samples on electric field, E_{dc} (The lines are just to guide the eyes)

overall pyroelectric activities of the samples. Amorin et al. (2000b) reported that the highest pyroelectric coefficient of sample LSBNT 5 could be obtained at 530 $\mu cm^{-2}K^{-1}$ as the sample had been sintered at the final stage (Amorin et al. 2000b; Amorin et al. 1999). The observed pyroelectric coefficients presented in lower value are mainly due to sintering temperature. Further explanation is discussed in SEM and XRD results.

Figure 6 shows the scanning electron micrographs of the samples. The sample LSBNT 1 before firing showed a high percentage of volume porosity which indicates the sintering process was at its early stage as shown in Figure 6a. Figures 6b, 6c and 6d show the SEM microstructure of the LSBNT 1, LSBNT 5 and LSBNT 10 compositions, respectively, which have been sintered at 1250°C for 5 h. The percentage of porosity for the sintered samples decreased due to lattice diffusion. Even though the compact ceramics with less percentage of porosity is observed in Figures 6b, 6c and 6d, the microstructure of the ceramic was already in its intermediate stage, where the voids from continuous pore channels along the grain

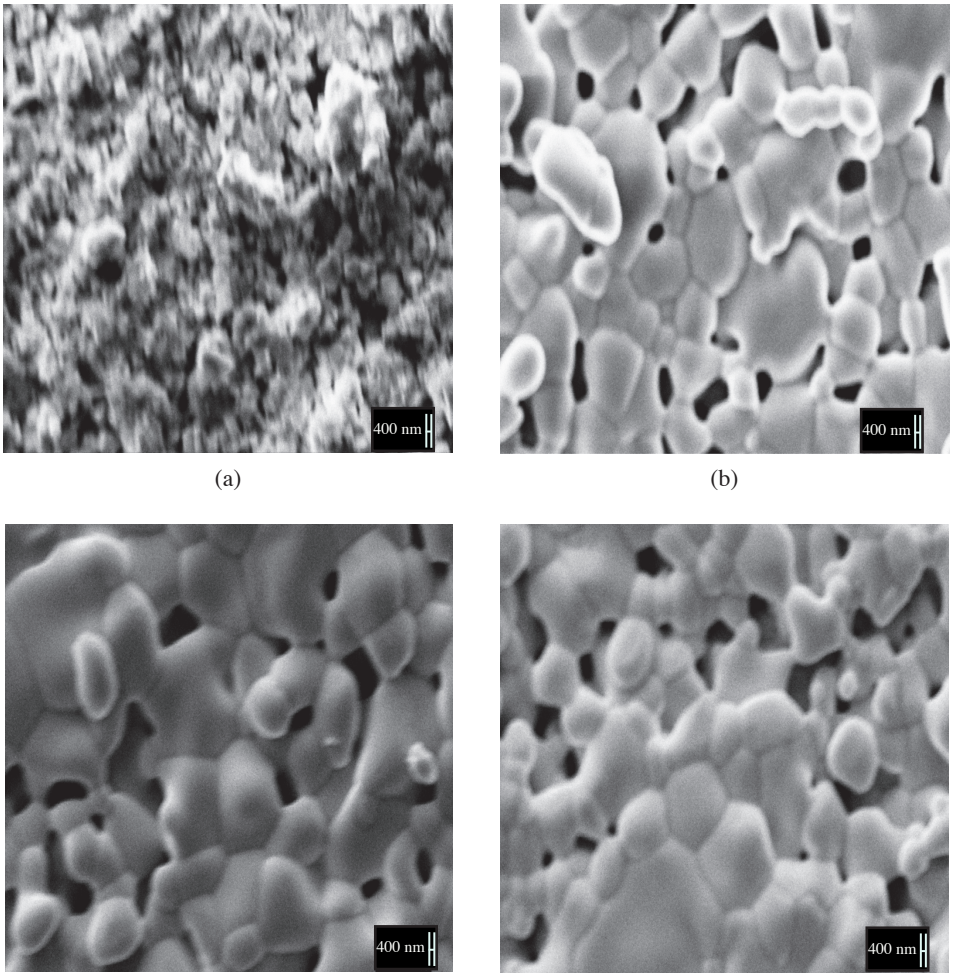

(a) (b)

(c) (d)

FIGURE 6. Scanning electron microstructure of sample (a) LSBNT 5 before sintering, (b) LSBNT 1, (c) LSBNT 5, (d) LSBNT 10 after sintered at 1250°C for 5 h

junctions become narrower. The microstructure of the samples sintered at 1250°C as shown in Figures 6b, 6c and 6d show a high density of interconnected pores indicative of the final stage of the sintering process is not yet achieved. As the sintering temperature keeps increasing, the densification proceeds and eventually discrete pores were formed when the overall porosity percentage decreased. Finally, the predominated long bar-shaped in the material formed as reported by Amorin et al. 2000a).

The mean grain size as obtained from the sintered samples shows a linear increase with respect to Ti concentration as shown in Figure 7. It can be seen that when the doping of Ti concentration was more than 0.07, the increase of mean grain size was gradual compared to that of Ti concentration < 0.07. Grain growth in dense materials is associated to grain boundary motion. The driving force of this mechanism is the lowering of the boundary energy by the ion motion through the grain boundary (Umakantham et al. 1996). Titanium substitution positively influenced the sintering process in the monophasics compositions region by increasing the grain boundary motion, the diffusion, densification kinetics that favor grain growth and the elimination of the porosity (Amorin et al. 2000a). The increasing of Ti percentage from 0.07 to 0.10 in the ceramics influenced the grain growth and the densification process. Consequently, the increase of mean grain size was gradual as the percentage of Ti concentration is above 0.07. These results coincide with the results presented by Amorin et al. (2000a) where the increase in Ti concentration in LSBNT ceramic from y = 0.01 to $y = 0.10$ leads to a linear increase in the ceramic mean grain size. The grain size of the particles as obtained from scanning electron microscope does not seem to give significant impact on the pyroelectric coefficient of the ceramic pellets.

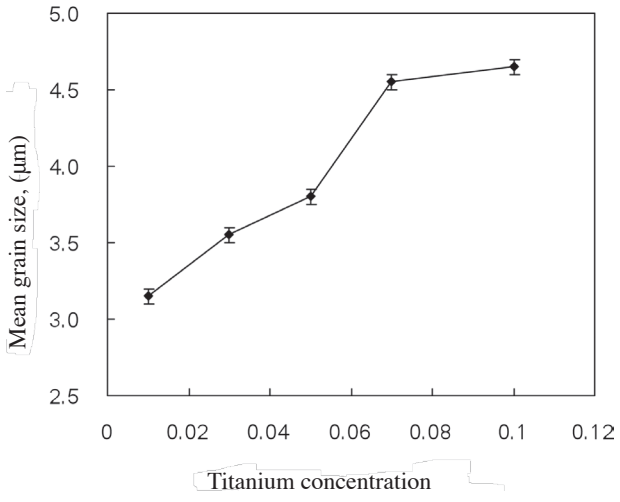

FIGURE 7. Mean grain size dependence with titanium concentration in samples sintered at 1250°C for 5 h

Figure 8 shows the XRD patterns for LSBNT samples with several Ti concentrations before and after sintering process at 1250°C for 5 h. A powder compact ceramic before it was fired, is composed of individual grains separated by 25 and 60 volume percentage porosity, depending on the particular material used and the processing method employed. In order to maximize the properties such as strength, translucency, and thermal conductivity, it is desirable to eliminate this porosity as much as possible. Therefore, the sintering process is important to reduce the compact porosity of the ceramic.

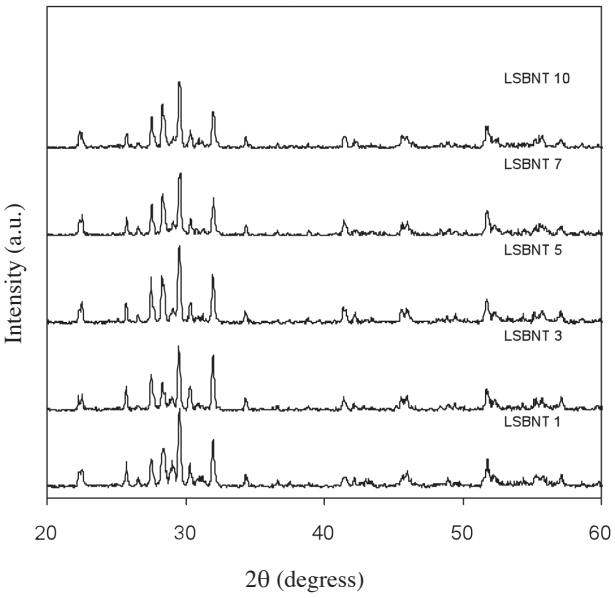

(a)

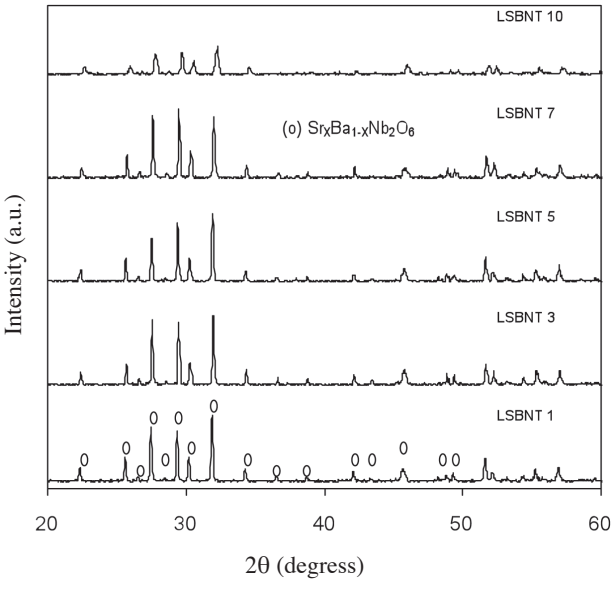

(b)

FIGURE 8. XRD patterns for $La_{0.03}Sr_{0.255}Ba_{0.7}Nb_{2-y}Ti_yO_{(6-y/2)}$ (LSBNT) ceramic samples with different titanium concentration (a) before sintering process and (b) after sintering process at 1250°C for 5 h

The sintering process is also widely used to increase the grain growth and to decrease the volume of isolated pores, to encourage the particle to approach the centre and increase overall densification, and inter-particle contact area with time. During the sintering process, the particle grain size grows as they become more spherical in shape and the pores between the particles are smaller in size due to the lattice diffusion (Chiang et al. 1997; Kingery et al. 1976). Hence, more intense XRD peaks are found in the samples which have been sintered. The mixture of the powders seems to diffuse as the sintering process were carried out at high temperature. However, the reflection peaks of the XRD patterns for all the LSBNT samples after sintering process elucidate that the mixtures of the various elements had yet not been completely diffused. A single phase compound is expected, and being isostructural with SBN phase after the sintering process (Amorin et al. 1999; Amorin et al. 2000b; Maciolek & Liu 1975). Yet, the reflection peaks of our XRD patterns which seem to coincide with the literature for SBN tetragonal tungsten bronze (TTB) structure (Jamieson et al. 1968) which reveals the LSBNT samples after sintering process exist as both mixture and compound phases. Once again, high density of interconnected pores and the absence of the predominated long bar-shaped in the material as observed by Amorin et al. 2000a) from our scanning electron micrographs validate our statement that the samples are not a single phase compound. The intermediate stage of sintering process which was applied to the LSBNT samples was dominated by the densification mechanisms. The densification mechanisms allow a large shrinkage of the open pores intersecting with the grain boundaries and thus reduce the overall mean porosity. As a consequence, the elements in the mixture were just partially diffused into the structure and as a result both mixture and compound phases were present in the ceramic.

Figure 9 shows the crystallite size of Ti and Nb inside the LSBNT sample which have been calculated by using Scherrer's equation from the XRD results. From Figure 7, it can be seen that both Ti and Nb crystallite size increases slightly and then decreases when the Ti concentration increases from $y = 0.01$ to 0.05 (LSBNT 1 to 5). The Nb crystallite size reaches its minimum value as the Ti concentration, $y = 0.05$ (LSBNT 5). This may explain why the sample with Ti, $y = 0.05$ exhibited the highest value of pyroelectric coefficient. LSBNT 5 has the lowest Nb crystallite size and also the second lowest of the Ti crystallite size. When the Ti concentration was increased further from $y = 0.07$ to 0.10 (LSBNT 7 to 10), the Ti crystallite size decreased dramatically from (58.0 ± 0.1) nm to (37.2 ± 0.1) nm. The crystallite size of Nb however increased from (35.9 ± 0.1) nm to (47.3 ± 0.1) nm and was much greater than the Ti crystallite size at this concentration. Even though the crystallite size of Ti at concentration $y = 0.10$ (LSBNT 10) is the lowest, the crystallite size of Nb is the highest. Therefore, the increase in the pyroelectric activity due to the decrease of Ti crystallite size has been suppressed by the increase of Nb crystallite size which resulted in the low pyroelectric coefficient of LSBNT 10.

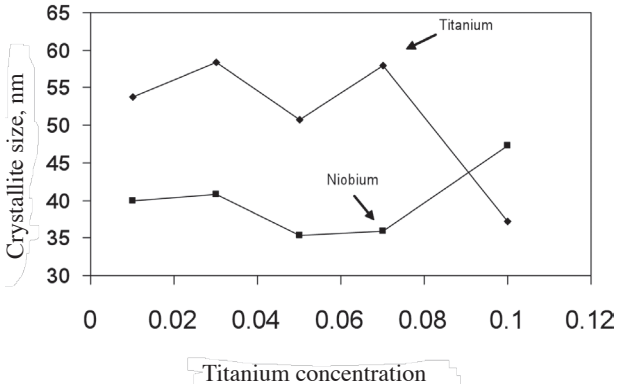

FIGURE 9. The dependence of crystallite size of Nb and Ti on the titanium concentration of the samples

CONCLUSIONS

The pyroelectric properties of $La_{0.03}Sr_{0.255}Ba_{0.7}Nb_{2-y}Ti_yO_{(6-y/2)}$ (LSBNT) ceramics depend on various applied electric field and crystallite size of Ti and Nb. In this work, E_{dc} of 20 kV cm^{-1} gives the highest pyroelectric activity. The increase of Ti concentration for $y > 0.05$ does not exhibit higher pyroelectric coefficient compared to the sample with Ti concentration of $y = 0.05$. This is because both of the crystallite sizes of Ti and Nb in these ceramic pellets after treated by sintering process influence the pyroelectric coefficient. The smaller the size of Ti and Nb crystallites, the higher is the pyroelectric coefficient of the LSBNT system. The size of Ti and Nb crystallites in LSBNT 5 is among the lowest compared to the other LSBNT samples. Therefore, the LSBNT 5 sample exhibited the highest pyroelectric coefficient among the samples because the crystallite size of Ti and Nb is the smallest.

REFERENCES

Abd Majid W.H. 1994. Pyroelectric activity in cyclic and linear polysiloxane Langmuir blodgett films. Ph.D. Thesis, University of Sheffield.

Amorin, H., Portelles, J., Guerrero, F., Fundora, A., Martinez, E. & Siqueiros, J.M. 2000a. Formation of the $La_{0.03}Sr_{0.255}Ba_{0.7}Nb_{2-y}Ti_yO_{(6-y)/2}$ ferroelectric system. *Journal of Materials Science* 35: 4607-4613.

Amorin, H., Portelles, J., Guerrero, F., Fundora, A. & Siqueiros, J. 1999. Formation properties of the $La_{0.03}Sr_{0.255}Ba_{0.7}Nb_{2-y}Ti_yO_{(6-y)/2}$ ceramic system. *Journal of Electroceramics* 3(4): 371-375.

Amorin, H., Portelles, J., Guerrero, F., Perez, J. & Siqueiros, J.M. 2000b. Dielectric hysteresis and pyroelectricity in the $La_{0.03}Sr_{0.255}Ba_{0.7}Nb_{2-y}Ti_yO_{(6-y)/2}$ ferroelectric ceramic system. *Solid State Communications* 113: 581-585.

Ares, J.R., Pascual, A., Ferrer, I.J. & Sanchez, C. 2005. Grain and crystallite size in polycrystalline pyrite thin films. *Thin Solid Films* 480-481: 477-481.

Calzada, M.L., Bretos, I., Jimenez, R., Ricote, J. & Mendiola, J. 2004. X-ray characterisation of chemical solution deposited $PbTiO_3$ films with high Ca doping. *Thin Solid Films* 450: 211.

Chiang, Y.M., D.P. Birnie, III, & Kingery, W.D. 1997. *Physical ceramics: Principles for Ceramic Science & Engineering*. New York: John Wiley & Sons, Inc.

Harrison, J.S. & Ounaies, Z. 2001. Piezoelectric polymers. *ICASE Report No. 2001-43*: 1-26.

Jamieson, P.B., Abrahams, S.C. & Bernstein, J.L. 1968. Ferroelectric Tungsten Bronze Type Crystal Structures. I. Barium Strontium Niobate $Ba_{0.27}Sr_{0.75}Nb_2O_{5.78}$. *J. Chem. Phys*. 48(11): 5048.

Kingery, W.D., Bowen, H.K. & Uhlmann, D.R. 1976. *Introduction to ceramics*. New York: John Wiley & Sons, Inc.

Kouchachvili, L. & Ikura, M. 2007. Pyroelectric conversion—Effects of P(VDF–TrFE) preconditioning on power conversion. *Journal of Electrostatics* 65: 182-188.

Lang, S.B. 2005. Pyroelectricity: From ancient curiosity to modern imaging tool. *Physics Today* 31-36.

Liete, E., Bernardi, M.I.B., Longo, E., Varela, J.A. & Paskocimas, C.A. 2004. Enhanced electrical property of nanostructured Sb-doped SnO_2 thin film processed by soft chemical method. *Thin Solid Films* 449: 67.

Liu, S.T. & Bhalla, A.S. 1983. Some interesting properties of dislocation free and La-modified $Sr_{0.5}Ba_{0.5}Nb_2O_6$. *Ferroelectrics* 51: 47-51.

Maciolek, R.B. & Liu, S.T. 1975. Preparation and physical properties of lanthanum-modified $Sr_{1-x}Ba_xNb_2O_6$ ferroelectric crystals. *Journal of Electronic Materials* 4: 571-526.

Nagata, K., Yamamoto, Y., Igarashi, H. & Okazaki, K. 1981. Properties of the hot-pressed strontium barium niobate ceramics. *Ferroelectrics* 38: 853-856.

Okada, K., Nagashima, T., Kameshima, Y. & Yasumori, A. 2003. Effect of crystallite size ofboehmite on sinterability of alumina ceramics. *Ceram. Int*. 29: 533.

Perez, J., Amorin, H., Portelles, J., Guerrero, F., M'Peko, J.C. & Siqueiros, J.M. 2001. Electrical properties of the titanium modified SBN ceramic system. *Journal of Electroceramics* 6(2): 153-157.

Rittidech, A. & Khotsongkram, P. 2006. Effect of ball milling times on phase formation of $Mg_{0.7}Zn_{0.3}Fe_2O_4$. *American Journal of Applied Sciences* 3(3): 1760-1762.

Umakantham, K. Chandramouli, K. Nageswara Rao, G. & Bhanumathi, A. 1996. *Bull. Mater. Sci*. 19(2): 345.

Xu, G., Zhang, Y.W., Liao, C.S. & Yan, C.H. 2004. Grain size-dependent electrical conductivity in scandia-stabilized zirconia prepared by a mild urea-based hydrothermal method. *Solid State Ionics* 166: 391.

Xu, Y. 1991. *Ferroelectric Materials and Their Applications* Los Angeles, USA: Elsevier Science (North-Holland).

Solid State Research Laboratory
Physics Department
University of Malaya
50603 Kuala Lumpur
Malaysia

*Corresponding author; email: wcgan1981@yahoo.com.sg

Received: 14 August 2009
Accepted: 1 April 2010